ELSEVIER

Contents lists available at ScienceDirect

Remote Sensing of Environment

journal homepage: www.elsevier.com/locate/rse





Fine-scale poverty estimation by integrating SDGSAT-1 glimmer images and urban functional zoning data[★]

Zejia Chen ^a, Huishan Luo ^a, Minting Li ^a, Jinyao Lin ^{a,*}, Xinchang Zhang ^{a,b,c,*}, Shaoying Li ^{a,*}

- ^a School of Geography and Remote Sensing, Guangzhou University, Guangzhou 510006, China
- ^b College of Geography and Remote Sensing Sciences, Xinjiang University, Urumqi 830046, China
- ^c Guangdong Urban and Rural Planning and Construction Intelligent Service Engineering Technology Research Center, Guangzhou 510290, China

ARTICLE INFO

Edited by Jing M. Chen

Keywords:
Poverty
SDGSAT-1
Urban functional area
Nighttime lights
Sustainable development
SDGs

ABSTRACT

Poverty is a pervasive global issue that adversely affects human well-being. Traditional socioeconomic censuses are time-consuming and resource-intensive, suffering from temporal delays, while reliance on nighttime light data with low spatial resolution is insufficient for fine-scale identification of impoverished regions. Furthermore, the spatial heterogeneity of nighttime light in different urban functional zones has been overlooked. To address these shortcomings, we proposed a novel approach by integrating high-resolution SDGSAT-1 nighttime light data (10 m) with urban functional zoning data using a spatial overlay tool. A random forest model was then applied to predict county-level poverty identification in Guangdong, China. For comparative validation, traditional NPP-VIIRS nighttime light data (500 m) were also incorporated. This method effectively explored the nonlinear relationship between nighttime light, urban functional zones, and the multidimensional poverty index (MPI, serving as the dependent variable). Our experiments demonstrate that the integration of urban functional zoning with nighttime light moderately improves the accuracy of poverty estimates. Among the models tested, the one considering functional zoning-based indicators of "number of light pixels" and "sum of pixel light values" increased the correlation coefficient by 0.0158 compared to the model without considering these indicators. Additionally, comparative analysis revealed that high-resolution data from SDGSAT-1 exhibited a better fit with the MPI when integrated with functional zoning-based indicators. Specifically, the correlation coefficient of this combination was 0.0086 higher than that of traditional NPP-VIIRS data. This highlights that SDGSAT-1 can delineate the boundaries between dark and light regions more precisely, leading to a more accurate reflection of regional poverty levels. Our findings facilitate fine-scale poverty estimation across large regions. This approach can inform policy design, such as dynamic optimization of resource allocation based on poverty estimates, thus enabling timely and accurate poverty alleviation efforts.

1. Introduction

Poverty is a pervasive worldwide phenomenon that poses significant challenges to human well-being (Ma et al., 2019; Meng et al., 2020; Rybnikova and Portnov, 2020). The Sustainable Development Goals proposed by the United Nations place a particular emphasis on the eradication of poverty. Poverty directly affects people's quality of life, social stability, and the development of countries (Gecchini et al., 2022; Pandey et al., 2022; Xu et al., 2021a). While a number of countries around the world have successfully addressed the issue of absolute poverty, there is still a need to continuously alleviate relative poverty

(Putri et al., 2022; Puttanapong et al., 2022; Su et al., 2017). Since relative poverty can be considered a multidimensional event, the development of quantitative models to measure relative poverty is a crucial and ongoing area of research (Hutasavi and Chen, 2022; Lin et al., 2022). The insights gained from these models can offer meaningful theoretical guidance for the design of poverty eradication projects (Jean et al., 2016; Wang et al., 2012).

The multidimensional poverty index (MPI) emerged as a key quantitative tool, capturing poverty's complexity through a three-level framework that goes beyond traditional income-based measures. According to the authoritative definition of the United Nations

 $^{^{\}star}$ This article is part of a Special issue entitled: 'SDGSAT-1 for SDGs' published in Remote Sensing of Environment.

^{*} Corresponding authors at: School of Geography and Remote Sensing, Guangzhou University, Guangzhou 510006, China. E-mail addresses: ljy2012@gzhu.edu.cn (J. Lin), zhangxc@gzhu.edu.cn (X. Zhang), lsy@gzhu.edu.cn (S. Li).

Development Programme (UNDP), poverty is essentially a dynamic three-dimensional system consisting of health deprivation, lack of education, and decline in quality of life (Gillis et al., 2001). This multidimensional conception encompasses not only the superficial dimension of income but also the restrictions on personal development opportunities (Schimmel, 2009). Notably, Alkire and Foster (2011) proposed the Alkire-Foster multidimensional poverty measurement theory, which was developed by selecting ten indicators from three dimensions. Hanandita et al. (2016) investigated the poverty condition in Indonesia according to earnings, health, and education. Liu and Xu (2016) developed a multidimensional indicator system based on the theory of sustainable livelihood framework, including financial, human, natural, and social capital elements, to assess rural poverty in China. However, the collection of traditional socioeconomic information is timeconsuming, and such statistical data are subject to delays that prevent timely updates on the poverty conditions (Asher et al., 2021; Elvidge et al., 2022; Liu et al., 2022; Tan et al., 2020).

Given its low cost and broad temporal and spatial coverage, nighttime light remote sensing has been demonstrated to effectively characterize timely and fine-scale socioeconomic conditions (Jia et al., 2024; Li et al., 2019; Zhang et al., 2019). For example, Chen et al. (2021a) employed a machine learning-based method to spatialize gross domestic product based on point of interest (POI) and nighttime light information. Bennett and Smith (2017) conducted a literature review and found that multitemporal nighttime light data are an appropriate proxy for socioeconomic indicators. In other fields, such as urban crime, Lee et al. (2024) investigated the relationship between nighttime crime and light values through univariate and multivariate analyses. Their findings showed that burglary exhibited the strongest correlation (R-squared value = 0.60) with nighttime light values, which emphasizes the utility of nighttime light data in urban crime analysis. Collectively, these studies have documented robust correlations between socioeconomic indicators and nighttime light information, while expanding their innovative applications in urban security monitoring and other areas. Current research trends indicate that nighttime light data are increasingly recognized as a crucial spatial analysis tool for understanding complex social issues.

A growing body of research has employed nighttime light data to identify impoverished regions (Coscieme et al., 2017; Li et al., 2020). For example, Elvidge et al. (2009) constructed a poverty index (PI) by dividing population count data by DMSP-OLS light brightness. They estimated worldwide poverty conditions based on the correlation between PI and DMSP-OLS light intensity. Yu et al. (2015) and Pan and Hu (2018) developed an average light index (ALI) and an average nighttime light index (ANLI), respectively, using NPP-VIIRS nighttime light data. They validated the correlation between these indices and actual poverty distribution through linear regression models to identify the spatial distribution of impoverished counties. However, these traditional nighttime remote sensing satellites are subject to the limitations of oversaturation and blooming effect (Guo et al., 2023b; Levin et al., 2020; Qiu et al., 2024; Zheng et al., 2023). Furthermore, the resolution of DMSP-OLS and NPP-VIIRS datasets is only 1000 m and 500 m, respectively, which is insufficient to support the urgent priority of accurate poverty alleviation (Hall et al., 2023; Zhao et al., 2022; Zhuo et al., 2018).

Interestingly, the Sustainable Development Goals Science Satellite 1 (SDGSAT-1), operated in 2021, provides data with high spatial resolution (10 m) and a large swath width of 300 km (Guo et al., 2023a). Its large swath width enables faster and more comprehensive coverage of large areas compared to traditional satellites (e.g., Landsat with 185 km swath width), thereby reducing temporal costs. The high resolution of SDGSAT-1 facilitates the identification of light distribution and microvariations within small rural settlements and towns. This feature overcomes the limitations of traditional data in fine-scale studies and mitigates blooming effects (Li et al., 2023a; Liu et al., 2024a). For example, SDGSAT-1 has demonstrated potential in extracting urban roads (Chang

et al., 2022; Wang et al., 2025b), identifying wetland (Xiang et al., 2023), exploring the spatial distribution of population (Duan et al., 2024; Liu et al., 2023a), investigating nighttime vitality (Xie et al., 2024), and evaluating light and air pollution (Lin et al., 2023; Liu et al., 2025). Moreover, the nighttime light product from SDGSAT-1 can be used to monitor poverty condition (Yu et al., 2023). Consequently, SDGSAT-1 is designed to provide more detailed information for socioeconomic research.

It is not necessarily the case that areas with low levels of nighttime brightness are experiencing poverty. Therefore, some research has addressed the limitations of nighttime light by combining multi-source geospatial data. For example, Shi et al. (2020) integrated topography, vegetation indices, POI, with nighttime light to recognize impoverished regions in Chongqing. Hu et al. (2022) combined POI, road network, and nighttime light to identify impoverished villages in Yunyang County. Li et al. (2023b) proposed a big data poverty indicator (BDPI) using nighttime light, POI, and house prices, which has the potential to replace the MPI. Niu et al. (2020) employed housing prices and nighttime light information to quantify urban poverty based on random forests. Li et al. (2024a) also considered the fusion of nighttime remote sensing and POI data for county-level regional development mapping in Wuling, China.

Nevertheless, previous studies have paid insufficient attention to the heterogeneity of nighttime brightness within different urban functional zones. Although some studies have attempted to combine multi-source data such as POI and road networks, they would benefit from a more systematic integration with urban functional zones. Liu et al. (2024b) revealed significant differences in lighting intensity and spectral characteristics across urban functional zones through the combination of field measurements and SDGSAT-1 nighttime light data. Lu et al. (2024) proposed a methodology for estimating electricity consumption by integrating Luojia 1-01 nighttime light data with urban functional zoning data. This method can accurately distinguish the power consumption patterns of industrial, residential, and other economic sectors. These studies demonstrate the effectiveness of urban functional zoning data in distinguishing the nighttime brightness of different economic sectors. While there is a paucity of studies that have explored the utility of urban functional zoning data in enhancing poverty estimation accuracy or fully leveraged their potential to characterize daytime economic vitality, related research has confirmed the capability of urban functional zoning to quantify spatiotemporal heterogeneity in human activities (Chen et al., 2022b; Cui et al., 2023; Du et al., 2024). This provides a more scientific basis for improving poverty estimation

To tackle the above weaknesses, this study was the first to integrate high-resolution SDGSAT-1 data with urban functional zoning data to explore their role in enhancing poverty estimation accuracy. The urban functional zoning data provide valuable insight into daytime socioeconomic activities and are beneficial for a more accurate differentiation in nighttime brightness characteristics across diverse economic sectors. This advantage enables a more comprehensive poverty estimation. For example, while secondary sector is vital to socioeconomic growth, the nighttime brightness of industrial parks may be relatively low. Furthermore, some public service facilities such as hospitals and libraries, which operate mainly during daytime hours, exhibit relatively low nighttime brightness. The incorporation of urban functional zoning data will enhance the comprehensiveness of poverty estimation. To this end, the non-linear association between the MPI and urban functional zoning-based indicators of nighttime light will be investigated.

The remainder of this paper is organized as follows: Section 2 introduces the study area, data sources, and the associated preprocessing steps. Section 3 describes the calculation method of the MPI, the construction of nighttime light indicators based on urban functional zoning, and the modeling process of random forest model. Section 4 presents the calculation results of the MPI, poverty estimation performance based on nighttime light and urban functional zoning, and identifies the optimal model through tenfold cross validation. Section 5 discusses the

differences in poverty estimation results across different data sources, analyzes the advantages and shortcomings of the proposed method, and offers policy recommendations. Section 6 summarizes the contributions of this study and outlines future research directions.

2. Data

2.1. Case study

Our research focuses on Guangdong Province of China, which comprises 122 counties within 21 prefecture-level cities. This province is situated in the southernmost part of the Chinese mainland. Since 1989, Guangdong has consistently ranked among the top provinces in China in terms of GDP. However, Guangdong Province has developed unevenly, with a concentration of impoverished counties in the eastern, western, and northern mountainous areas. These regions are affected by their location and topographical conditions, resulting in a notable lag in socioeconomic development compared with the Pearl River Delta. Fig. 1 illustrates the considerable variation in county-level GDP across the whole province.

2.2. Socioeconomic indicators

In accordance with the sustainable livelihoods framework established by previous studies and the availability of data, this study adopted 14 socioeconomic indicators from diverse aspects: economy, health, education, livelihood, and environment (Table 1) (Chen et al., 2022a; Li et al., 2024a; Pan and Hu, 2018; Pokhriyal and Jacques, 2017). These indicators were integrated to construct the MPI, which serves as a comprehensive tool for identifying impoverished counties.

Data acquisition is limited by timeliness constraints. According to the Guangdong Statistical Yearbook and Population Census data, Guangdong Province experienced no substantial socioeconomic structural changes during 2020–2022. Therefore, the study period for socioeconomic indicators was set to this period, which can balance data availability and research timeliness while ensuring the robustness of the MPI.

Table 1
Socioeconomic indicators of MPI.

Dimension	Indicator	Source	Year	Resolution
Economy	Gross regional product	Guangdong Statistical	2020	-
	Proportion of	Yearbook	2020	_
	secondary and			
	tertiary industries			
	Density of	POI of AutoNavi	2022	-
	companies and	Map		
	enterprises			
Health	Medical and health institutions	Guangdong Social Statistical	2020	_
	insututions	Yearbook		
Education	Years of schooling	Guangdong	2020	_
		Provincial		
		Population Census		
Livelihood	Density of scientific,	POI of AutoNavi	2022	-
	educational, and	Map		
	cultural service			
	facilities	Cuanadana	2020	
	Housing area per capita	Guangdong Provincial	2020	_
	capita	Population Census		
	Road density	OpenStreetMap	2022	_
	Average house price	Anjuke and Loupan	2022	_
		Platforms		
	Density of living and	POI of AutoNavi	2022	-
	leisure service	Map		
	facilities		2022	
	Density of transportation		2022	_
	service facilities			
Environment	Average slope	NASA DEM	_	30 m
	Average terrain	https://www.geo	-	1000 m
	relief	doi.ac.cn		
	Average rainfall	National	-	1000 m
		Meteorological		
		Information Center		

2.3. SDGSAT-1 data

The nighttime light products of SDGSAT-1 (Fig. 2a) are characterized by multiple bands (RGB and panchromatic) and high spatiotemporal resolution (Table 2), which can provide finer information for

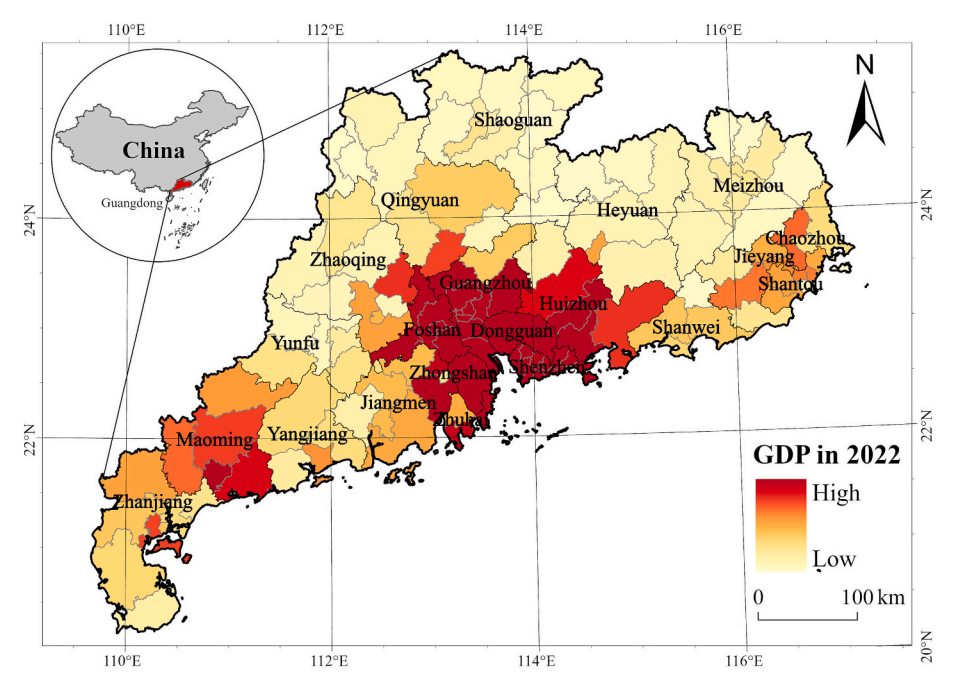


Fig. 1. County-level GDP of Guangdong in 2022.

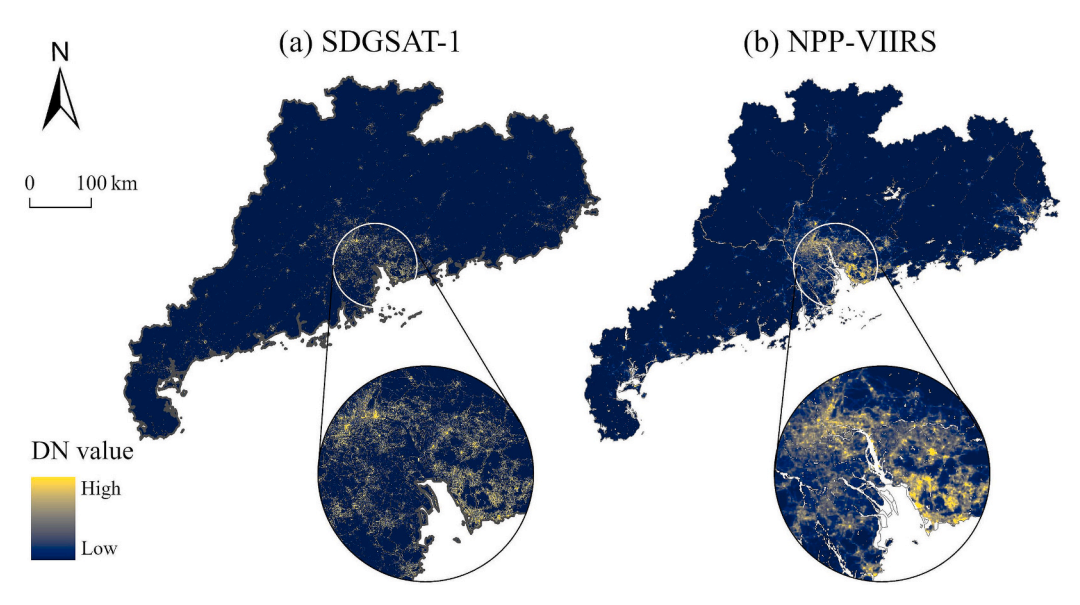


Fig. 2. SDGSAT-1 and NPP-VIIRS data in Guangdong.

Table 2
Comparison between SDGSAT-1 and NPP-VIIRS.

	SDGSAT-1	NPP-VIIRS
Spatial resolution	10 m	500 m
Swath width	300 km	3000 km
Availability	2021-now	2012-now

socioeconomic monitoring (Yu et al., 2023). Since the original product of SDGSAT-1 still exhibits noise, noise removal and radiometric calibration were conducted in accordance with previous research. To distinguish between noises and regular pixels, appropriate thresholds were established based on the distribution patterns of the noises. Specifically, the image was first binarized. Then, a customized filter was devised to eliminate the noisy regions with pixel connectivity less than 5 in the binary image, while retaining the regions with connectivity greater than 5. Further details regarding noise removal and radiometric calibration can be found in the articles of Liu et al. (2024a) and Zhang et al. (2022).

Image processing techniques, including de-blooming algorithms and functions in image processing software, are commonly employed to tackle the oversaturation and blooming effect (Bai et al., 2023). Our study mainly adopted the threshold truncation method to mitigate the blooming effect and noise by setting thresholds. Noise removal can significantly reduce stripe and salt-and-pepper noise while minimizing information loss. In addition, radiometric calibration can convert original digital values into physical quantities, providing an accurate basis for quantitative analysis. Collectively, these processes indirectly alleviate both oversaturation and blooming phenomena, thereby enhancing data quality and enabling detailed information extraction (Liu et al., 2023b; Wang et al., 2025a; Zhang et al., 2022).

2.4. NPP-VIIRS data

The NPP-VIIRS data (Fig. 2b) were collected from the joint NASA/NOAA programs (Sanchez de Miguel et al., 2020; Stokes and Roman, 2022; Zhao et al., 2020). A well-calibrated and preprocessed product in 2022 was obtained from the National Earth System Scientific Data Platform (https://geodata.nnu.edu.cn/). This widely-used product was generated through the fusion of data from NPP-VIIRS and DMSP-OLS (Chen et al., 2021b). First, the enhanced vegetation index (EVI) was used to adjust the DMSP-OLS nighttime light data to mitigate saturation

effects and amplify variations in light intensity. Then, a convolutional neural network (CNN)-based autoencoder model was developed to extract high-order image features from the adjusted DMSP-OLS data and map them to the feature space of NPP-VIIRS data, which enables the simulation of nighttime light data similar to NPP-VIIRS data. This process addressed discrepancies between the satellite sensors in terms of resolution, radiometric calibration, and temporal coverage, creating a nighttime light dataset with a long time span and consistency.

2.5. Urban functional zoning data

In this study, the spatial heterogeneity of nighttime light within different urban functional zones was carefully considered. For this purpose, the urban functional zoning product in 2018 was obtained from the China Urban Land Use Mapping Research Group (Gong et al., 2020). This dataset classifies cities into five types: residential, commercial, industrial, transportation, and public management and utilities (Fig. 3). These classifications were generated through a random forest algorithm integrating multi-source geospatial data (Sentinel-2 imagery, POIs, and nighttime lights).

3. Method

First, the MPI was established based on the socioeconomic indicators presented in Table 1, and several nighttime light indicators (Table S1) were calculated within each urban functional zone. Second, a correlation assessment was performed between all nighttime light indicators and the MPI at a county scale. The highly relevant indicators were then subjected to multicollinearity diagnosis. Third, a series of random forest models were constructed with different combinations of the remaining nighttime light indicators. Tenfold cross validation was used to identify the optimal combinations. The results were further compared with those of the traditional methods to examine the performance of our method (Fig. 4).

3.1. Multidimensional poverty index

The initial step was to standardize the 14 socioeconomic indicators presented in Table 1. Subsequently, the data were reduced in dimension through principal component analysis, and the KMO and Bartlett's assessments were performed. A KMO value exceeding 0.6 signifies that the principal component analysis is effective. The variance contribution ratio of each component was divided by the cumulative contribution

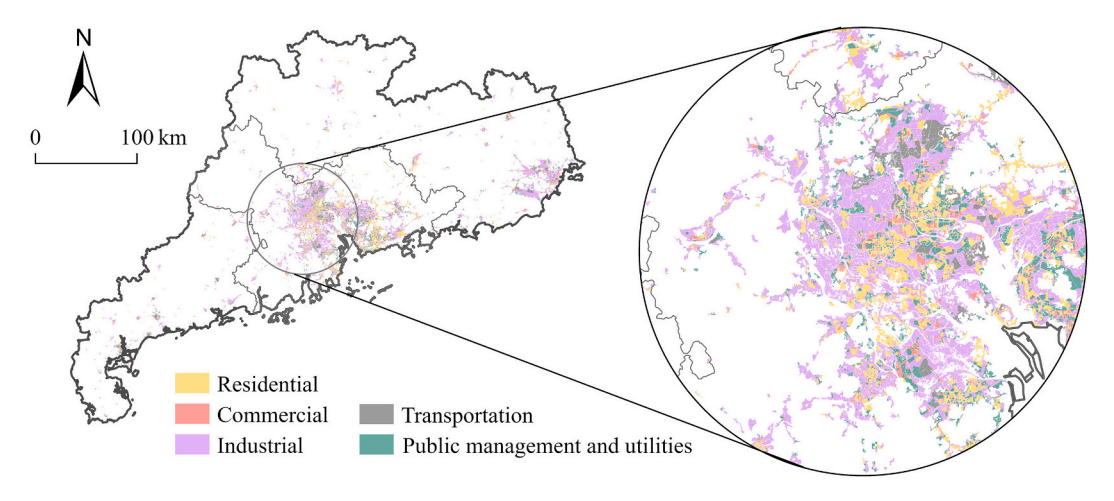


Fig. 3. Urban functional zoning in Guangdong.

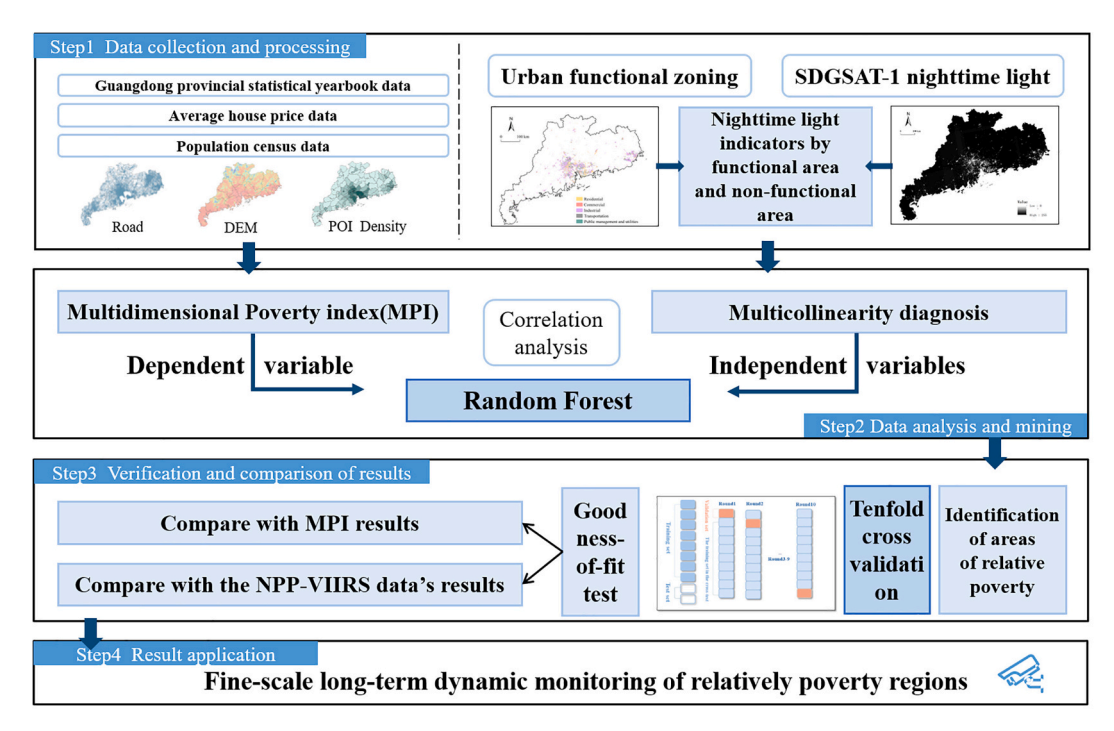


Fig. 4. Poverty estimation using nighttime light and urban functional zoning.

ratio to determine the weight of each indicator. Ultimately, county-level MPIs were calculated to reflect the poverty condition of each county as follows:

$$MPI = \sum_{i=1}^{14} w_i \times x_i \tag{1}$$

where x_i is the score of the *i*-th metric; w_i is the weight for the *i*-th metric.

3.2. Urban functional zoning-based nighttime light indicators

It has been demonstrated by previous research that the fusion of nighttime light and urban land use information can substantially improve the spatialization of socioeconomic indicators (Chen et al., 2016; Lu et al., 2024; Wei et al., 2021). Accordingly, urban functional zoning data were employed to complement daytime information on socioeconomic activities. By considering the nighttime light features of diverse urban functional zones, it is expected that a more comprehensive

estimation of poverty can be achieved. In accordance with previous outcomes (Li et al., 2021; Luo et al., 2022; Xu et al., 2021c; Yin et al., 2021; Zheng et al., 2024), twelve categories of nighttime light characteristics were quantified from four perspectives (central tendency, dispersion degree, distribution characteristic, and spatial characteristic) (Table S1).

First, the county-level nighttime light characteristics of the entire study area (i.e., nighttime light indicators without considering urban functional zoning) were calculated using the SDGSAT-1 nighttime light data in isolation. Subsequently, the nighttime light characteristics within each urban functional zone were calculated at the county level. This was achieved by combining urban functional zoning data with nighttime light using a spatial overlay tool (i.e., nighttime light indicators considering urban functional zoning). To facilitate comparison with the SDGSAT-1 data, the same operation was applied to the NPP-VIIRS nighttime light product.

3.3. Random forest

Random forest is a powerful machine learning technique that can accurately perform data regression and classification tasks, as well as address missing values (Chen et al., 2021a; Hu et al., 2022; Niu et al., 2020). The random forest model is based on multiple decision trees, each constructed independently, which allows for the effective solution of high-dimensional and nonlinear problems by combining all the decision trees. Therefore, it can effectively handle missing data, non-equilibrium conditions, and multicollinearity in the dataset. It offers advantages such as resistance to overfitting, fast computation, and the ability to achieve usable results without fine-tuning parameters. In several poverty estimation comparison studies, random forest has outperformed other machine learning models (Chen et al., 2025; Muñetón-Santa and Manrique-Ruiz, 2023; Yin et al., 2021; Zheng et al., 2024).

In this study, a series of random forest models were constructed to identify the nonlinear relationship between the MPI (dependent variable) and nighttime light characteristics (SDGSAT-1/NPP-VIIRS) (independent variables). A tenfold cross validation rule was employed to examine the effectiveness of these models. This operation was iterated ten times, and the mean validation metrics of different models were calculated to identify the optimal combination of independent variables. To assess the model's predictive capability and generalization performance, five metrics, including correlation coefficient, average absolute error, root mean square error, relative absolute error, and relative square root error, were used.

4. Results

4.1. MPI

The KMO score is 0.846, and the significance of Bartlett's assessment is less than 0.05. These results suggest that there is a moderate to high correlation between the variables, which makes them suitable for principal component analysis. The associated weighting outcomes are presented in Table 3.

Accordingly, the county-level MPIs in Guangdong Province were calculated using Eq. (1). To provide a more illustrative representation of the geographical distribution of poverty conditions, a natural break rule (Jenks) was employed to categorize the MPI values as five levels: very low (0.00–0.20), low (0.21–0.25), moderate (0.26–0.35), high (0.36–0.45), and very high (0.46–0.8) (Fig. 5). Specifically, a lower MPI level indicates a more severe poverty condition. In accordance with the findings of previous studies, the counties with a very low MPI level were classified as impoverished counties, and the same applies to the poverty level (Pan and Hu, 2018; Xu et al., 2021b; Yin et al., 2021).

The MPI results are found to be consistent with the actual poverty condition. In particular, the peripheral counties in Guangdong Province

Table 3 Weighting for socioeconomic indicators.

Indicator	Attribute	Weight
Gross regional product	+	0.0989
Percentage of secondary and tertiary industries	+	0.0576
Density of companies and enterprises	+	0.0844
Medical and health institutions	+	0.0781
Years of schooling	+	0.0638
Density of scientific, educational, and cultural service	+	0.0687
facilities	-	0.0551
Housing area per capita	+	0.0751
Road density	+	0.0802
Average house price	+	0.0683
Density of living and leisure service facilities	+	0.0744
Density of transportation service facilities	-	0.0687
Average slope	-	0.0721
Average terrain relief	+	0.0541
Average rainfall		

are facing greater challenges in combating poverty. The impoverished counties were typically situated in the eastern and northern parts of this province, including Maoming, Yunfu, Zhaoqing, Yangjiang, Shaoquan, and Heyuan, which are geographically more remote. In contrast, the more developed counties clustered in Guangzhou, Shenzhen, and Foshan, which are the cores of Guangdong's socioeconomic development.

4.2. Poverty estimation based on nighttime light and urban functional zoning

For the sake of clarity, the nighttime light indicators calculated without urban functional zoning are referred to as "basic indicators" hereafter. First, a correlation analysis was conducted between all indicators and the MPI to exclude those that did not exhibit a significant correlation. Second, a multicollinearity diagnosis was performed on the remaining basic indicators, which resulted in the exclusion of those with significant multicollinearity (VIF > 10).

To test the hypothesis that the basic indicators are significantly correlated with the MPI, a Pearson correlation analysis was conducted. The null hypothesis (no correlation, $\rho=0$) was evaluated using a two-tailed significance test. Fig. 6 illustrates the outcomes of the hypothesis testing for the correlation between the selected basic indicators and the MPI. The Pearson correlation analysis revealed a significant correlation between all basic indicators and the MPI, thereby allowing us to reject the null hypothesis ($\rho=0$) at the 5 % significance level.

After performing multicollinearity diagnosis and correlation analysis, the retained basic indicators were combined with each single functional zoning-based nighttime light indicator. The performance of these different combinations was quantified through tenfold cross validation (Table 4). The results demonstrate that the models considering the following five additional indicators performed better than the model using only the basic indicators.

First, the "sum of pixel light values" can depict the degree of socioeconomic development at night and shows a strong correlation with poverty conditions. Second, the "median of pixel light values" is less susceptible to the influence of outliers and provides a robust measure of central tendency. This makes it an effective tool for capturing the disparity between wealth and poverty. Third, the "mode of pixel light values" reflects the most common brightness levels and thus reveals the type of socioeconomic activity that dominates this region. Fourth, the "number of light pixels" is correlated with population and economic size, reflecting the coverage of socioeconomic activities. Fifth, the "local Moran index" measures the heterogeneity of the spatial distribution of light brightness, which is also a key indicator of impoverished counties. Notably, compared with the "average light index" that reflects the average brightness, the "sum of pixel light values" and "number of light pixels" can better capture the light distribution characteristics within different functional zones. Our results show that the correlation coefficients of the models considering the "sum of pixel light values" and "number of light pixels" are as high as 0.9463 and 0.9450, respectively.

The five high-performance indicators derived from the above screening were subsequently combined in pairs (Table 5). Results show that the model combining the basic indicators with the "sum of pixel light values" and "number of light pixels" indicators achieves the highest accuracy. Specifically, a region may exhibit a high total light value concentrated in a limited number of pixels (e.g., urban cores), while a large number of light pixels may indicate broader spatial coverage of economic activities (e.g., suburban areas). A moderate total light value, accompanied by an abundance of light pixels, may indicate dispersed moderate development. Conversely, a high total light value with sparse light pixels could signify centralized development. The combination of these two indicators enables the model to simultaneously capture both the overall intensity and spatial coverage of nighttime illumination. Consequently, this combination achieves a correlation coefficient that is 0.0158 higher than the result obtained using only the basic indicator.

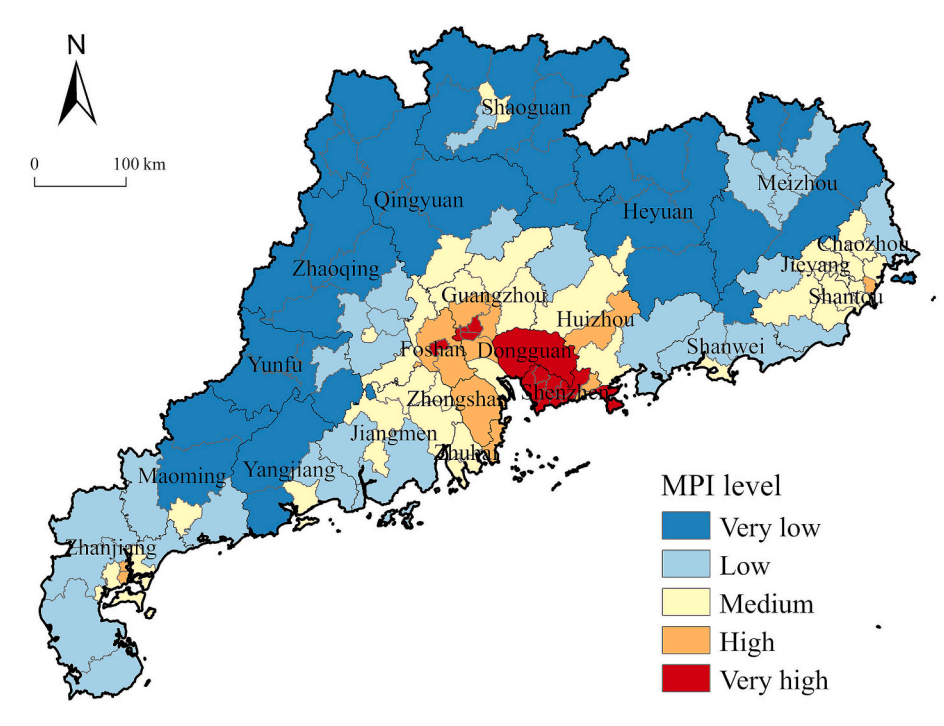


Fig. 5. Spatial distribution of MPI level in Guangdong.

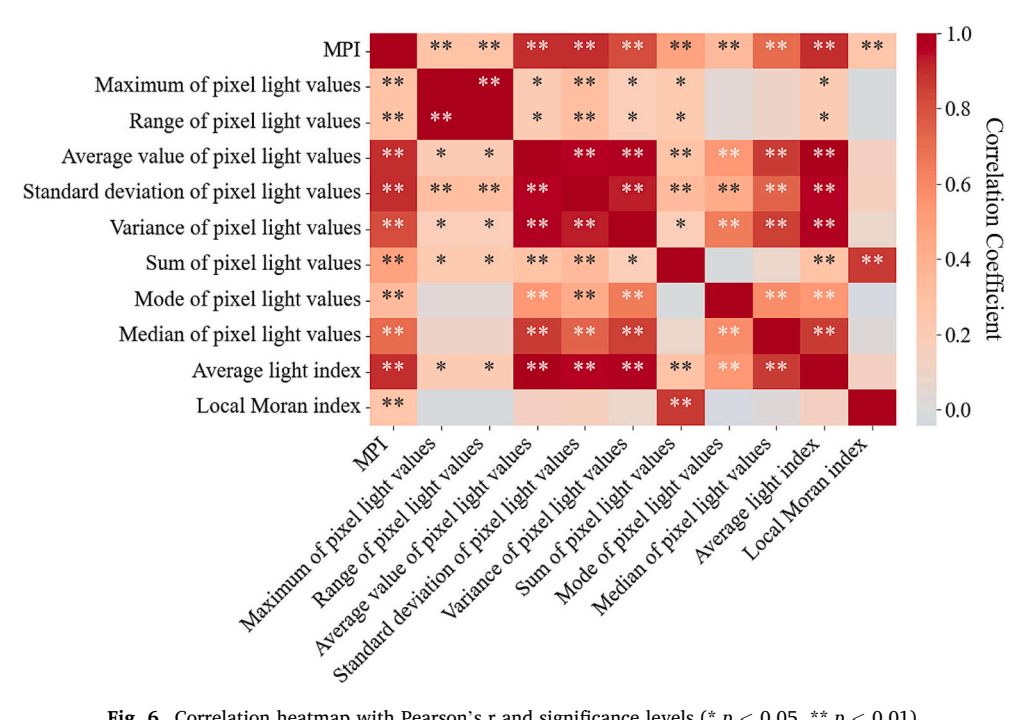


Fig. 6. Correlation heatmap with Pearson's r and significance levels (* p < 0.05, ** p < 0.01).

Linear regression analysis was performed to examine the association between the model's predicted outcomes and the MPI. Fig. 7a presents the scatter plot and regression line ($v = 0.8002 \times + 0.0515$, $R^2 = 0.8767$) for the model using only SDGSAT-1 basic indicators. The high ${\rm R}^2$ value demonstrates a strong alignment between model predictions and MPI values, indicating an accurate representation of actual poverty

For the optimal model identified through tenfold cross validation, which combines the SDGSAT-1 basic indicators with the "sum of pixel light values" and "number of light pixels" indicators, Fig. 7b shows improved performance (y = $0.7750 \times + 0.0547$, R² = 0.8949). This model exhibits a stronger explanatory power for the variations in the MPI, accounting for approximately 89.49 % of the changes. These results further validate the statistically significant correlation between the combined model's predictions and the MPI. It indicates that the combined model, which contains more comprehensive nighttime light information, aligns better with the actual situation.

To enhance the clarity of the optimal model (integrating SDGSAT-1 basic indicators, the "sum of pixel light values", and the "number of light pixels"), a SHAP (Shapley Additive Explanation) value analysis was conducted. As illustrated in Fig. 8, the three most influential positive indicators are the "average value of pixel light values" (SHAP value =

Table 4Results of combining basic indicators with each single functional zoning-based nighttime light indicator (SDGSAT-1).

Combining basic indicators with the following functional zoning-based indicator	Correlation coefficient	Average absolute error	Root mean square error	Relative absolute error (%)	Relative square root error (%)
_	0.9342	0.0362	0.0482	36.3673	35.9438
Sum of pixel light values	0.9463	0.0338	0.0457	33.9339	34.1121
Number of light pixels	0.9450	0.0302	0.0458	30.3055	34.1383
Local Moran Index	0.9432	0.0332	0.0458	33.3027	34.1586
Mode of pixel light values	0.9383	0.0358	0.0468	35.9778	34.9232
Median of pixel light values	0.9366	0.0357	0.0480	35.8438	35.7864
Minimum of pixel light values	0.9329	0.0363	0.0486	36.4173	36.2555
Variance of pixel light values	0.9322	0.0364	0.0497	36.5301	37.1129
Average light index	0.9312	0.0356	0.0495	35.7766	36.9047
Average value of pixel light values	0.9312	0.0356	0.0495	35.7766	36.9047
Maximum of pixel light values	0.9304	0.0362	0.0502	36.2905	37.4314
Standard deviation of pixel light values	0.9292	0.0363	0.0510	36.4265	38.0573
Range of pixel light values	0.9291	0.0369	0.0504	37.0475	37.5693

Note (same below): The first row shows the results obtained using only the basic indicators. The numbers in bold indicate that the results are superior to those obtained using only the basic indicators. Basic indicators refer to those calculated using only nighttime light data, while functional zoning-based indicators are calculated by integrating nighttime light data with urban functional zoning data.

0.02241), "sum of pixel light values in the commercial zone" (SHAP value = 0.01788), and "sum of pixel light values" (SHAP value = 0.01548). These indicators collectively reflect the overall economic conditions and highlight areas of robust development. In contrast, the "sum of pixel light values in the public management and utilities zone" (SHAP value = 0.00859), "number of light pixels in the public management and utilities zone" (SHAP value = 0.00810), and "sum of pixel light values in the residential zone" (SHAP value = 0.00793) compensate for the relatively low nighttime light values in these functional zones, thereby effectively capturing their daytime economic activity levels. This integrated spatiotemporal analysis enables the model to effectively interpret both daytime and nighttime economic patterns, thereby enhancing the clarity of poverty estimation.

For further comparison, the NPP-VIIRS data were also utilized to estimate poverty conditions in Guangdong Province. All steps were identical to those described above for the SDGSAT-1 data. The results presented in Tables S2 and S3 further confirm the validity of the combination of the basic indicators, the "sum of pixel light values", and "number of light pixels".

Table 5Results of combining basic indicators with multiple functional zoning-based nighttime light indicators (SDGSAT-1).

8					
Combining	Correlation	Average	Root	Relative	Relative
basic	coefficient	absolute	mean	absolute	square
indicators		error	square	error (%)	root error
with the			error		(%)
following					
functional					
zoning-based					
indicators					
-	0.9342	0.0362	0.0482	36.3673	35.9438
Sum of pixel	0.9500	0.0311	0.0443	31.2270	33.0876
light values					
&					
Number of					
light pixels					
Number of	0.9476	0.0301	0.0465	30.2585	34.6855
light pixels					
&					
Local					
Moran Index					
Median of	0.9467	0.0340	0.0471	34.1653	35.1382
pixel light					
values &					
Local					
Moran Index					
Sum of pixel	0.9447	0.0328	0.0472	32.9131	35.2194
light values					
&					
Local					
Moran Index					
Number of	0.9446	0.0307	0.0464	30.8255	34.5934
light pixels					
&					
Median of					
pixel light					
values					
Mode of pixel	0.9433	0.0325	0.0466	32.5916	34.7313
light values					
&					
Local					
Moran Index					
Number of	0.9420	0.0320	0.0470	32.1080	35.0535
light pixels					
&					
Mode of					
pixel light					
values					
Sum of pixel	0.9408	0.0332	0.0478	33.3008	35.6890
light values					
&					
Mode of					
pixel light					
values					
Sum of pixel	0.9402	0.0343	0.0483	34.4575	36.0206
light values					
&					
Median of					
pixel light					
values					
Mode of pixel	0.9341	0.0360	0.0498	36.1308	37.1894
light values					
&					
Median of					
pixel light					
values					

5. Discussion

5.1. Comparison of poverty estimation results

To further validate our method, a spatial comparison between the outcomes derived from the nighttime light and the MPI was conducted (Fig. 9). The results were reclassified in accordance with the MPI levels depicted in Fig. 5, and counties with values below 0.2 were considered

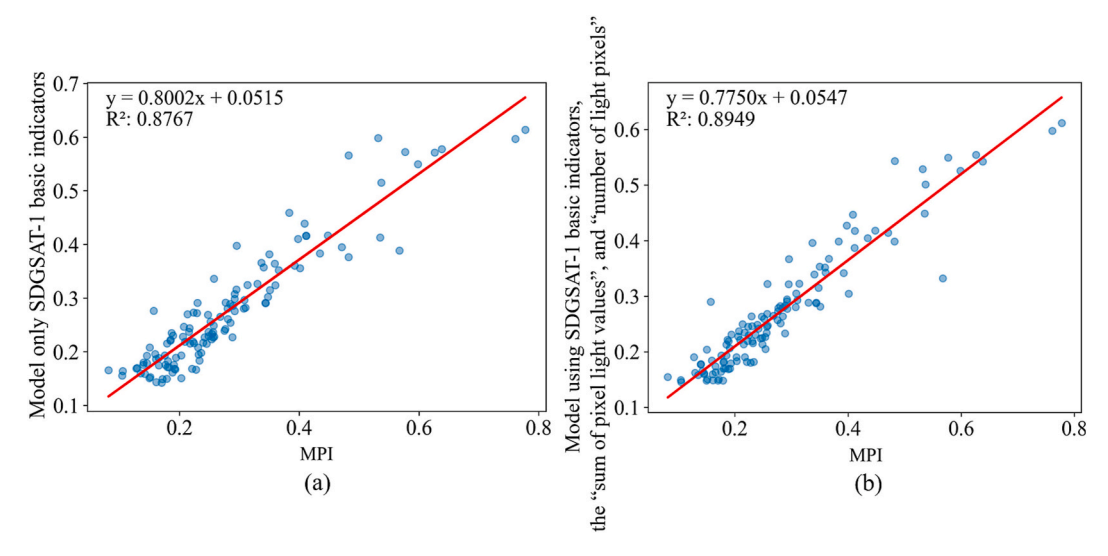


Fig. 7. Regression between the model's predicted outcomes and the MPI: (a) using only SDGSAT-1 basic indicators; (b) using SDGSAT-1 basic indicators, the "sum of pixel light values", and "number of light pixels".

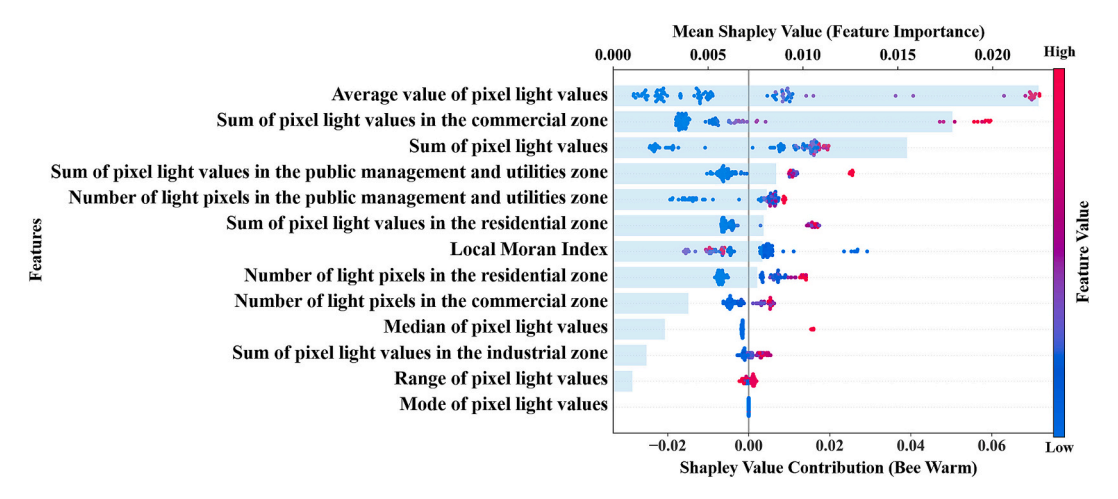


Fig. 8. SHAP values of the model using SDGSAT-1 basic indicators, the "sum of pixel light values", and "number of light pixels".

impoverished counties. Overall, the impoverished counties recognized via our method are broadly consistent with the results derived from the MPI. The discrepancies between the two are typically distributed in the northern and western parts of Guangdong. Specifically, the impoverished counties that were predicted to be non-impoverished were mainly Qujiang, Yangxi, and Xinxing, while the non-impoverished counties that were predicted to be impoverished were mainly Leizhou, Xingning, and Meixian.

The calculation of the MPI is highly dependent on reliable statistical data. Although statistical yearbooks provide valuable data for socioeconomic analyses, they are limited by their update frequency and statistical units. In economically developed regions with impoverished subregions, these limitations may result in an incomplete and potentially inaccurate estimation. In contrast, nighttime light data, as one of the informative indicators for measuring socioeconomic activities at a fine scale, better capture the differences in human activities at night. Additionally, the incorporation of functional zoning-based indicators is advantageous for reflecting the spatial heterogeneity in economic activities and social services across various urban functional zones. For example, industrial zones may exhibit low nighttime brightness due to limited operations at night but generate significant economic output during the day. Residential and public management and utilities zones (e.g., schools, hospitals), which typically have lower nighttime light

intensity but are critical for quality of life, align with MPI dimensions such as education and health. Our functional zoning-based indicators (e. g., "sum of pixel light values in the industrial zone") complement these daytime economic activities. Consequently, the use of these indicators enables the indirect capture of crucial information on daytime socioeconomic activities, thereby facilitating a more comprehensive poverty estimation.

Among the four methods, the results derived from the combination of the SDGSAT-1 basic indicators with the functional zoning-based indicators exhibited the greatest consistency with the MPI. For instance, Fogang was incorrectly identified as an impoverished county in all three other results. In fact, Fogang exhibits spatial mixing of industrial and residential zones in some regions. In the model using NPP-VIIRS basic indicators, the "sum of pixel light values", and "number of light pixels", the benefits of functional zoning were undermined by the coarse resolution of NPP-VIIRS, which hindered effective identification of mixed land use patterns. Conversely, the model using only SDGSAT-1 basic indicators can leverage its 10 m resolution to detect small-scale light variations. However, this model lacks functional zoning information, making it difficult to distinguish low-brightness industrial zones from actual impoverished regions. Similarly, the model using only NPP-VIIRS basic indicators tends to misclassify Fogang's scattered public service facilities as impoverished regions due to their low nighttime brightness,

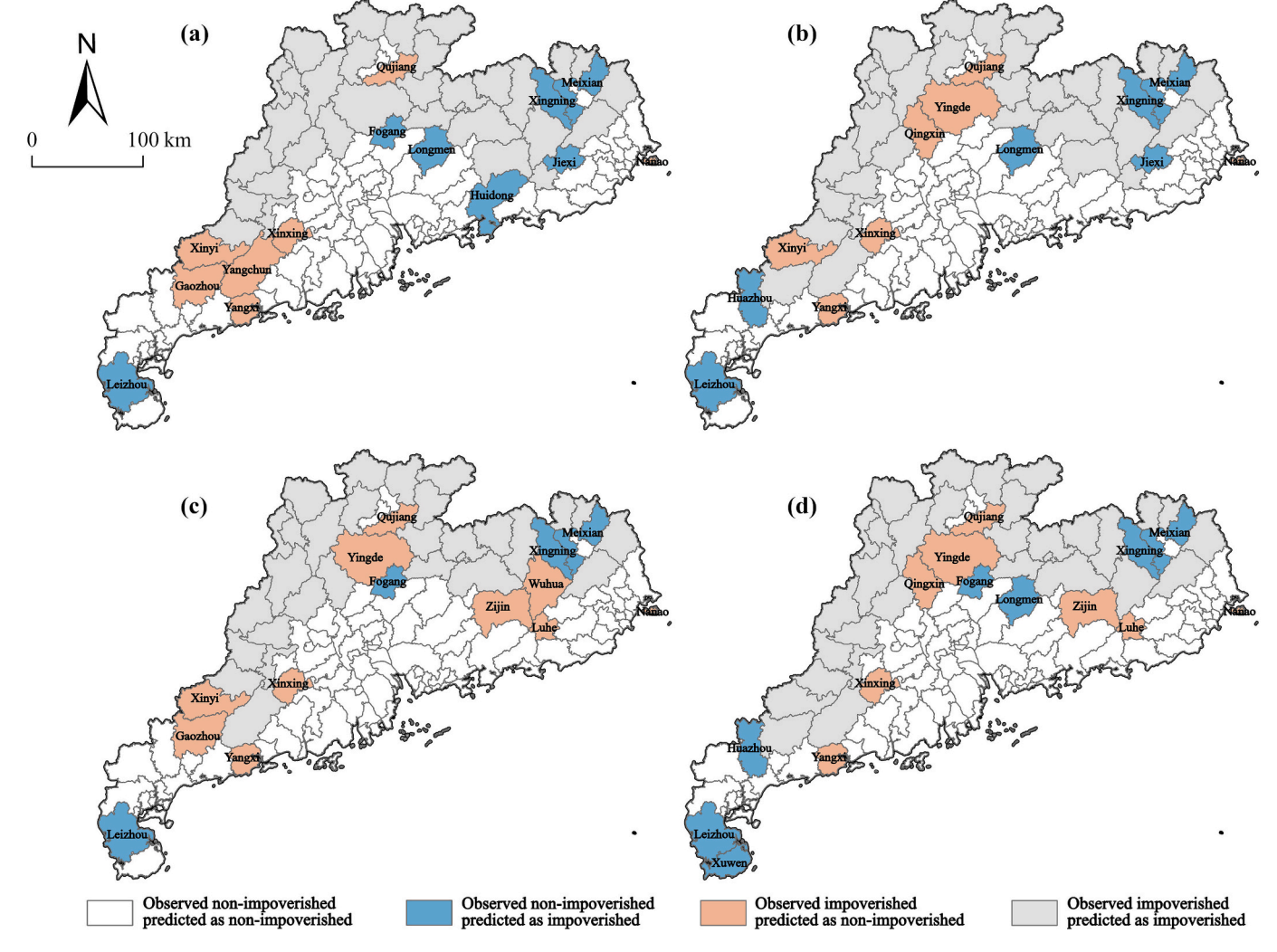


Fig. 9. Comparison between MPI and the results of nighttime light: (a) using only SDGSAT-1 basic indicators; (b) using SDGSAT-1 basic indicators, the "sum of pixel light values", and "number of light pixels"; (c) using only NPP-VIIRS basic indicators; (d) using NPP-VIIRS basic indicators, the "sum of pixel light values", and "number of light pixels".

leading to incorrect classifications.

Furthermore, the poverty level results obtained through the above four methods were compared (Fig. 10). In all four results, there is a noticeable decrease in poverty level from the center to the periphery of Guangdong Province, with the northern part of the province exhibiting a relatively low poverty level. The results obtained without considering the functional zoning-based indicators (Fig. 10a and Fig. 10c) were unable to identify the impoverished counties in Maoming. In comparison, the results including the functional zoning-based indicators (Fig. 10b and Fig. 10d) were more consistent with the results of the MPI, which further supports the reasonableness of our proposed method.

Our further investigation has revealed that the inclusion of urban functional zoning can alleviate this limitation associated with high-resolution nighttime light data. Functional zoning-based indicators effectively differentiate brightness characteristics across economic sectors, thereby enabling adequate reflection of daytime activity areas. After considering these new indicators (Fig. 9b and Fig. 10b), some areas that were initially misclassified as impoverished counties were corrected. For counties with concentrated nighttime light in specific areas, the remaining parts with low nighttime light can be characterized by the "number of light pixels" and "sum of pixel light values" within different functional zones. These two additional indicators provide essential information on the extent of light coverage and the sum of light values for each functional zone. Nevertheless, for large areas with concentrated

development (e.g., Dongguan City without subordinate counties), the aforementioned issues may still lead to misclassification of poverty levels.

Finally, the performance of the SDGSAT-1 data with the NPP-VIIRS data regarding poverty estimation was compared. Without considering functional zoning-based indicators, SDGSAT-1 (Fig. 10a) identified fewer counties with medium, high, and very high poverty levels than NPP-VIIRS (Fig. 10c). For example, the results from SDGSAT-1 showed lower poverty levels in Panyu District of Guangzhou and Guangming District of Shenzhen. The high resolution of SDGSAT-1 enables it to capture finer nighttime light variations, but it may also be oversensitive to low-brightness areas (e.g., parks, industrial zones). In contrast, NPP-VIIRS suffers from blooming effect, and its low resolution leads to widespread overestimation of brightness values (e.g., urban center brightness diffusing to suburban areas), thereby underestimating the number of impoverished counties. This discrepancy indicates that while SDGSAT-1's high resolution enhances the accuracy of poverty identification, its sensitivity to low-light areas requires auxiliary calibration with functional zoning data. NPP-VIIRS, despite its high temporal resolution and low computational cost, is limited in mixed-functional zones due to insufficient spatial precision. Therefore, the combination of these two data sources offers a more comprehensive perspective for poverty estimation.

After incorporating functional zoning-based indicators, NPP-VIIRS

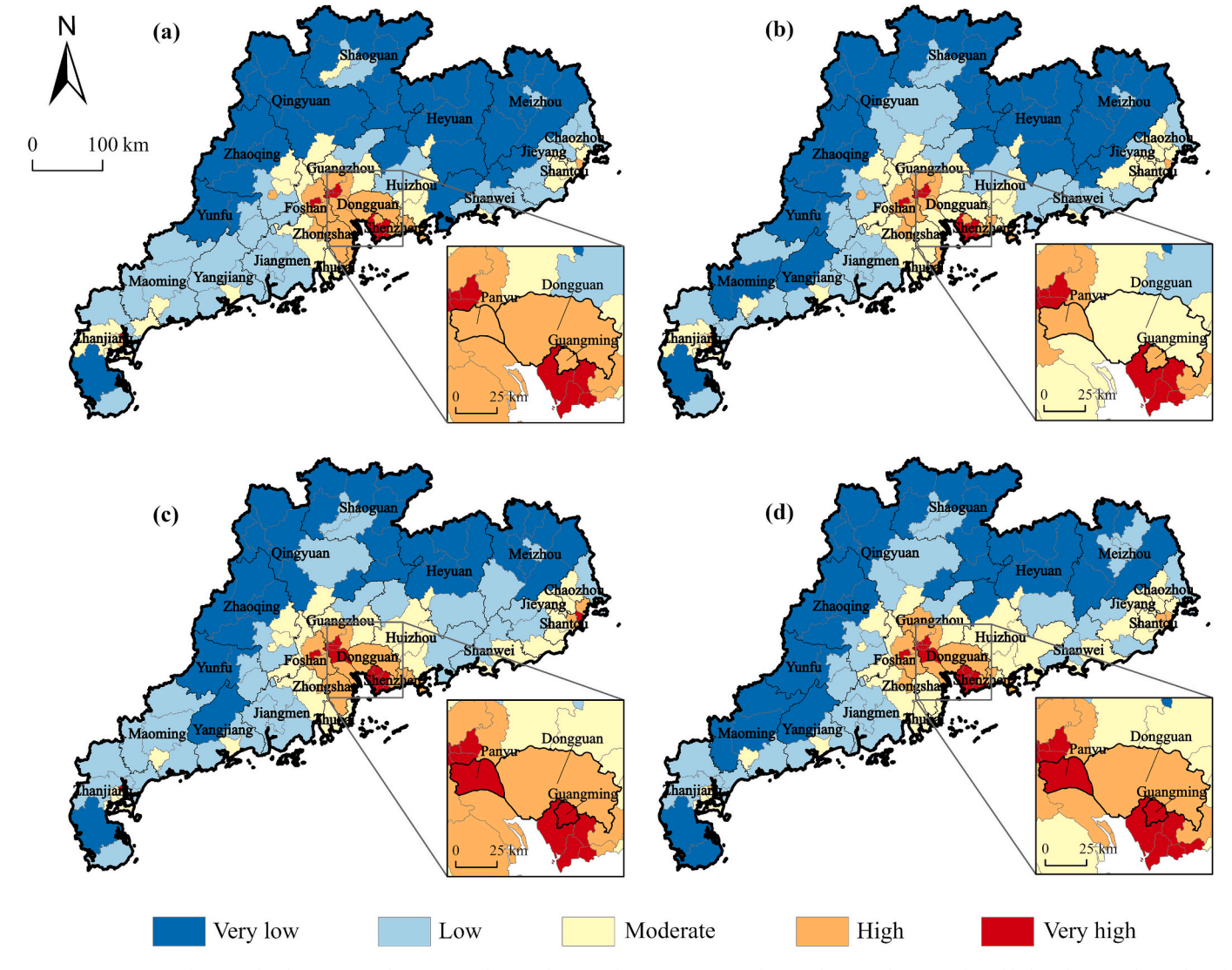


Fig. 10. Comparison of poverty level: (a) using only SDGSAT-1 basic indicators; (b) using SDGSAT-1 basic indicators, the "sum of pixel light values", and "number of light pixels"; (c) using only NPP-VIIRS basic indicators; (d) using NPP-VIIRS basic indicators, the "sum of pixel light values", and "number of light pixels".

identified more impoverished counties accurately (Fig. 9c and Fig. 9d), with the correlation coefficient of its model increasing by 0.0129. However, NPP-VIIRS still struggles to delineate the edges between dark and light regions precisely due to inherent limitations (Li et al., 2024b; Ma et al., 2014; Ni et al., 2021; Zhang et al., 2015). Therefore, its improvement in correlation coefficient was 0.0029 lower than that of SDGSAT-1. These results indicate that functional zoning indicators enhance poverty estimation for both datasets. Nevertheless, the models demonstrated higher performance when integrated with the higher-resolution SDGSAT-1 data.

5.2. Advantages and shortcomings of this study

The above comparisons support the validity of the methodology proposed in this study. Compared with the approaches that rely solely on nighttime light data, this methodology has carefully accounted for regional spatial heterogeneity. The reasonableness of the poverty estimation results can be improved by incorporating urban functional zoning-based indicators. In summary, the proposed methodology offers two key advantages. First, the use of high spatiotemporal resolution SDGSAT-1 nighttime light data provides a solution to the delays and coarse units of statistical data. Second, the inclusion of urban functional zoning information allows for a more accurate distinction between the

light brightness characteristics of different economic sectors, thereby providing a more comprehensive approach to poverty estimation.

In light of our findings, three policy recommendations can be made for the alleviation of poverty. First, it is imperative that local governments accurately identify regions experiencing relative poverty and devise differentiated poverty reduction strategies based on regional characteristics. In particular, it is essential to strengthen the sustainable development and risk-resistance capacity of economically disadvantaged regions, including those in the eastern, western, and northern parts of Guangdong. For impoverished counties with single-functional zoning, priority should be given to investing in infrastructure for characteristic industries. Second, local governments need to implement a long-term dynamic tracking system to enhance the responsiveness and accuracy of poverty alleviation policies. For example, in similar poverty zones identified by the model (e.g., Liannanyaozu in Qingyuan and Ruyuanyaozu in Shaoguan), the effectiveness of characteristic industries (e.g., eco-tourism) in poverty alleviation can be evaluated by integrating changes in nighttime light intensity with industrial income data. Finally, local governments can establish an early warning mechanism for poverty trends in accordance with the methodology of this study. By identifying poverty clusters through modeling results and spatial autocorrelation analysis, emergency industrial funds can be allocated regularly. Implementing early intervention measures based on poverty estimation results can prevent the phenomenon of "returning to poverty" in Guangdong Province.

It should also be acknowledged that the poverty estimation model developed in this study has some shortcomings, as the urban functional zoning data employed is solely based on the 2018 mapping results. First, the data on transportation areas could not be incorporated into the model due to a considerable number of missing values. It would be beneficial for future studies to obtain more complete information. Second, using county as the unit of analysis may not fully reflect the differences in sub-regional development within the county. Finally, the acquisition and updating of functional zoning data face significant challenges (Hu et al., 2024; Tang et al., 2022; Xiong et al., 2025; Zhang et al., 2025). These challenges include high costs and processing complexities for high-resolution data, which results in delayed updates, illdefined boundaries, and incomplete spatial coverage. A finer unit, such as grid-scale resolution, could be employed in future attempts to gain a more complete picture of poverty conditions. This could be complemented by more timely data (e.g., mobile phone signaling data) to quantify daytime population mobility and economic activity hotspots.

6. Conclusions

This study aims to explore the potential of integrating high-resolution SDGSAT-1 data with urban functional zoning data to estimate poverty. It addresses two critical challenges: the insufficient timeliness of traditional socioeconomic statistical data and the limited ability of coarse-resolution remote sensing products to characterize spatial heterogeneity. The results show that the model combining functional zoning-based indicators of "sum of pixel light values" and "number of light pixels" demonstrated the highest degree of effectiveness.

Specifically, this research contributes to the literature in two distinct aspects. First, the SDGSAT-1 data with a resolution of 10 m were employed for poverty estimation, which can strengthen the reliability of the fitting outcomes. The high temporal resolution of these data provides an opportunity for long-term dynamic monitoring on a large scale, which is beneficial for accurately alleviating poverty and promoting urban-rural integration. Second, an integrated use of nighttime light and urban functional zoning effectively distinguishes the nighttime light characteristics across diverse economic sectors. This novel combination can account for regional spatial heterogeneity and offer an ideal basis for the accurate identification of impoverished regions. In conclusion, our findings have great potential to support fine-scale poverty estimation over a wide area. Although county-scale models may exhibit biases in large areas with concentrated development, future studies will involve acquiring more timely data (e.g., mobile phone signaling data), adopting a more refined grid scale, and expanding the study area to urban agglomerations such as the Yangtze River Delta and Beijing-Tianjin-Hebei region. These efforts aim to provide valuable insights for targeted poverty alleviation, enhance poverty monitoring, and support evidencebased policy-making.

CRediT authorship contribution statement

Zejia Chen: Writing – original draft, Formal analysis. Huishan Luo: Methodology, Formal analysis, Data curation. Minting Li: Visualization, Validation. Jinyao Lin: Writing – review & editing, Resources, Methodology. Xinchang Zhang: Writing – review & editing, Supervision. Shaoying Li: Project administration, Funding acquisition.

Declaration of competing interest

The authors declare that they have no known competing financial interests or personal relationships that could have appeared to influence the work reported in this paper.

Acknowledgement

This study was funded by Guangdong Philosophy and Social Science Foundation (Grant No. GD23XSH11), and National College Students Innovation and Entrepreneurship Training Program (Grant No. 202411078005), and Humanities and Social Sciences Research Program of the Ministry of Education of China (Grant No. 23YJCZH125), and National Natural Science Foundation of China (Grant No. 42430515, 42271467, 42371406). The research findings are a component of the SDGSAT-1 Open Science Program, which is conducted by the International Research Center of Big Data for Sustainable Development Goals (CBAS). The data utilized in this study is sourced from SDGSAT-1 and provided by CBAS.

Appendix A. Supplementary data

Supplementary data to this article can be found online at https://doi.org/10.1016/j.rse.2025.114925.

Data availability

Data will be made available on request.

References

- Alkire, S., Foster, J., 2011. Counting and multidimensional poverty measurement. J. Public Econ. 95, 476–487.
- Asher, S., Lunt, T., Matsuura, R., Novosad, P., 2021. Development research at high geographic resolution: an analysis of night-lights, firms, and poverty in India using the SHRUG open data platform. World Bank Econ. Rev. 35, 845–871.
- Bai, X., Li, X., Miao, J., Shen, H., 2023. Making the earth clear at night: a high-resolution Nighttime light image Deblooming network. IEEE Trans. Geosci. Remote Sensing 61, 1–13.
- Bennett, M.M., Smith, L.C., 2017. Advances in using multitemporal night-time lights satellite imagery to detect, estimate, and monitor socioeconomic dynamics. Remote Sens. Environ. 192, 176–197.
- Cecchini, S., Savio, G., Tromben, V., 2022. Mapping poverty rates in Chile with night lights and fractional multinomial models. Reg. Sci. Policy Pract. 14, 850–877.
- Chang, D., Wang, Q., Yang, J., Xu, W., 2022. Research on road extraction method based on sustainable development goals Satellite-1 Nighttime light data. Remote Sens 14, 6015
- Chen, Q., Hou, X., Zhang, X., Ma, C., 2016. Improved GDP spatialization approach by combining land-use data and night-time light data: a case study in China's continental coastal area. Int. J. Remote Sens. 37, 4610–4622.
- Chen, Q., Ye, T., Zhao, N., Ding, M., Ouyang, Z., Jia, P., Yue, W., Yang, X., 2021a. Mapping China's regional economic activity by integrating points-of-interest and remote sensing data with random forest. Environment and Planning B: Urban Analytics and City Science 48, 1876–1894.
- Chen, Z., Yu, B., Yang, C., Zhou, Y., Yao, S., Qian, X., Wang, C., Wu, B., Wu, J., 2021b. An extended time series (2000-2018) of global NPP-VIIRS-like nighttime light data from a cross-sensor calibration. Earth Syst. Sci. Data 13, 889–906.
- Chen, R., Zhang, F., Chan, N.W., Wang, Y., 2022a. Multidimensional poverty measurement and spatial-temporal pattern analysis at county level in the arid area of Xinjiang, China. Environ. Dev. Sustain. 25, 13805–13824.
- Chen, Y., Yang, J., Yang, R., Xiao, X., Xia, J., 2022b. Contribution of urban functional zones to the spatial distribution of urban thermal environment. Build. Environ. 216, 109000.
- Chen, Z., Zhang, C., Qiu, S., Lin, J., 2025. GDP estimation by integrating Qimingxing-1 Nighttime light, street-view imagery, and points of interest: an empirical study in Dongguan City. Remote Sens 17, 1127.
- Coscieme, L., Sutton, P.C., Anderson, S., Liu, Q., Elvidge, C.D., 2017. Dark times: nighttime satellite imagery as a detector of regional disparity and the geography of conflict. GISc. & Remote Sens. 54, 118–139.
- Cui, Y., Zha, H., Jiang, L., Zhang, M., Shi, K., 2023. Luojia 1–01 data outperform Suomi-NPP VIIRS data in estimating CO_2 emissions in the service, industrial, and urban residential sectors. IEEE Geosci. Remote Sensing Lett. 20, 1–5.
- Du, S., Zhang, Y., Sun, W., Liu, B., 2024. Quantifying heterogeneous impacts of 2D/3D built environment on carbon emissions across urban functional zones: a case study in Beijing, China. Energy and Buildings 319, 114513.
- Duan, H., Shi, Z., Ge, J., Wu, F., Liu, Y., Zhang, H., Wang, C., 2024. High-resolution population mapping based on SDGSAT-1 glimmer imagery and deep learning: a case study of the Guangdong-Hong Kong-Marco Greater Bay Area. Int. J. Digit. Earth 17, 2407519.
- Elvidge, C.D., Sutton, P.C., Ghosh, T., Tuttle, B.T., Baugh, K.E., Bhaduri, B., Bright, E., 2009. A global poverty map derived from satellite data. Comput. Geosci. 35, 1652–1660.

- Elvidge, C.D., Baugh, K., Ghosh, T., Zhizhin, M., Hsu, F.C., Sparks, T., Bazilian, M., Sutton, P.C., Houngbedji, K., Goldblatt, R., 2022. Fifty years of nightly global lowlight imaging satellite observations. Front. Remote Sens. 3, 919937.
- Gillis, M., Shoup, C., Sicat, G.P., 2001. World Development Report 2000/2001 -Attacking Poverty.
- Gong, P., Chen, B., Li, X., Liu, H., Wang, J., Bai, Y., Chen, J., Chen, X., Fang, L., Feng, S., Feng, Y., Gong, Y., Gu, H., Huang, H., Huang, X., Jiao, H., Kang, Y., Lei, G., Li, A., Li, X., Li, X., Li, Y., Li, Z., Liu, C., Liu, C., Liu, M., Liu, S., Mao, W., Miao, C., Ni, H., Pan, Q., Qi, S., Ren, Z., Shan, Z., Shen, S., Shi, M., Song, Y., Su, M., Ping, Suen, H., Sun, B., Sun, F., Sun, J., Sun, L., Sun, W., Tian, T., Tong, X., Tseng, Y., Tu, Y., Wang, H., Wang, L., Wang, X., Wang, Z., Wu, T., Xie, Y., Yang, J., Yang, J., Yuan, M., Yue, W., Zeng, H., Zhang, K., Zhang, N., Zhang, T., Zhang, Y., Zhoo, F., Zheng, Y., Zhou, Q., Clinton, N., Zhu, Z., Xu, B., 2020. Mapping essential urban land use categories in China (EULUC-China): preliminary results for 2018. Sci. Bull. 65, 182–187.
- Guo, H., Dou, C., Chen, H., Liu, J., Fu, B., Li, X., Zou, Z., Liang, D., 2023a. SDGSAT-1: the world's first scientific satellite for sustainable development goals. Sci. Bull. 68, 34–38
- Guo, W., Zhang, J., Zhao, X., Li, Y., Liu, J., Sun, W., Fan, D., 2023b. Combining Luojia1-01 Nighttime light and points-of-interest data for fine mapping of population spatialization based on the zonal classification method. IEEE J. Sel. Top. Appl. Earth Observations Remote Sensing 16, 1589–1600.
- Hall, O., Dompae, F., Wahab, I., Dzanku, F.M., 2023. A review of machine learning and satellite imagery for poverty prediction: implications for development research and applications. J. Int. Dev. 35, 1753–1768.
- Hanandita, W., Tampubolon, G., Maggino, F., 2016. Multidimensional Poverty in Indonesia: Trend over the Last Decade (2003–2013).
- Hu, S., Ge, Y., Liu, M., Ren, Z., Zhang, X., 2022. Village-level poverty identification using machine learning, high-resolution images, and geospatial data. Int. J. Appl. Earth Obs. Geoinf. 107, 102694.
- Hu, Z., Chu, Y., Zhang, Y., Zheng, X., Wang, J., Xu, W., Wang, J., Wu, G., 2024. Scale matters: how spatial resolution impacts remote sensing based urban green space mapping? Int. J. Appl. Earth Obs. Geoinf. 134, 104178.
- Hutasavi, S., Chen, D., 2022. Exploring the industrial growth and poverty alleviation through space-time data mining from night-time light images: a case study in eastern economic corridor (EEC), Thailand. Int. J. Remote Sens. 45, 7803–7825.
- Jean, N., Burke, M., Xie, M., Davis, W.M., Lobell, D.B., Ermon, S., 2016. Combining satellite imagery and machine learning to predict poverty. Science 353, 790–794.
- Jia, M., Zeng, H., Chen, Z., Wang, Z., Ren, C., Mao, D., Zhao, C., Zhang, R., Wang, Y., 2024. Nighttime light in China's coastal zone: the type classification approach using SDGSAT-1 glimmer imager. Remote Sens. Environ. 305, 114104.
- Lee, J., Leitner, M., Paulus, G., 2024. Spatiotemporal analysis of Nighttime crimes in Vienna. Austria. ISPRS Int. J. Geo-Inf. 13, 247.
- Levin, N., Kyba, C.C.M., Zhang, Q., Sánchez de Miguel, A., Román, M.O., Li, X., Portnov, B.A., Molthan, A.L., Jechow, A., Miller, S.D., Wang, Z., Shrestha, R.M., Elvidge, C.D., 2020. Remote sensing of night lights: a review and an outlook for the future. Remote Sens. Environ. 237, 111443.
- Li, X., Li, X., Li, D., He, X., Jendryke, M., 2019. A preliminary investigation of Luojia-1 night-time light imagery. Remote Sens. Lett. 10, 526–535.
 Li, C., Yang, W., Tang, Q., Tang, X., Lei, J., Wu, M., Qiu, S., 2020. Detection of
- Li, C., Yang, W., Tang, Q., Tang, X., Lei, J., Wu, M., Qiu, S., 2020. Detection of multidimensional poverty using Luojia 1-01 Nighttime light imagery. J. Indian Soc. Remote Sens. 48, 963–977.
- Li, G., Cai, Z., Qian, Y., Chen, F., 2021. Identifying urban poverty using high-resolution satellite imagery and machine learning approaches: implications for housing inequality. Land 10.
- Li, C., Chen, F., Wang, N., Yu, B., Wang, L., 2023a. SDGSAT-1 nighttime light data improve village-scale built-up delineation. Remote Sens. Environ. 297, 113764.
- Li, M., Lin, J., Ji, Z., Chen, K., Liu, J., 2023b. Grid-scale poverty assessment by integrating high-resolution Nighttime light and spatial big data—a case study in the Pearl River Delta. Remote Sens 15, 4618.
- Li, L., Hu, T., Yang, G., He, W., Zhang, H., 2024a. High-resolution comprehensive regional development mapping using multisource geographic data. Sustain. Cities Soc. 113, 105670.
- Li, X., Liu, S., Ma, Q., Cao, W., Zhang, H., Wang, Z., 2024b. Impacts of spatial explanatory variables on surface urban heat island intensity between urban and suburban regions in China. International Journal of Digital Earth 17, 2304074.
- Lin, J., Luo, S., Huang, Y., 2022. Poverty estimation at the county level by combining LuoJia1-01 nighttime light data and points of interest. Geocarto Int. 1–17.
- Lin, Z., Jiao, W., Liu, H., Long, T., Liu, Y., Wei, S., He, G., Trop, T., Portnov, B.A., Liu, M., Li, X., Wen, C., 2023. Modelling the public perception of urban public space lighting based on SDGSAT-1 glimmer imagery: a case study in Beijing. China. Sust. Cities Soc. 88. 104272.
- Liu, Y., Xu, Y., 2016. A geographic identification of multidimensional poverty in rural China under the framework of sustainable livelihoods analysis. Appl. Geogr. 73, 62–76.
- Liu, H., Wang, J., Liu, H., Chen, Y., Liu, X., Guo, Y., Huang, H., 2022. Identification of relative poverty based on 2012-2020 NPP/VIIRS night light data: in the area surrounding Beijing and Tianjin in China. Sustainability 14, 5559.
- Liu, C., Chen, Y., Wei, Y., Chen, F., 2023a. Spatial population distribution data disaggregation based on SDGSAT-1 Nighttime light and land use data using Guilin, China, as an example. Remote Sens 15, 2926.
- Liu, Y., Long, T., Jiao, W., Chen, B., Cheng, B., Du, Y., He, G., Huang, P., 2023b. Leveraging "night-day" calibration data to correct stripe noise and vignetting in SDGSAT-1 Nighttime-light images. IEEE Trans. Geosci. Remote Sensing 61, 1–23.
- Liu, S., Wang, C., Chen, Z., Li, W., Zhang, L., Wu, B., Huang, Y., Li, Y., Ni, J., Wu, J., Yu, B., 2024a. Efficacy of the SDGSAT-1 glimmer imagery in measuring sustainable

- development goal indicators 7.1.1, 11.5.2, and target 7.3. Remote Sens. Environ. 305, 114079.
- Liu, S., Zhou, Y., Wang, F., Wang, S., Wang, Z., Wang, Y., Qin, G., Wang, P., Liu, M., Huang, L., 2024b. Lighting characteristics of public space in urban functional areas based on SDGSAT-1 glimmer imagery: A case study in Beijing, China. Remote Sens. Environ. 306, 114137.
- Liu, X., Lu, L., Guo, H., Li, Z., Li, X., Bilal, M., 2025. Evaluating fine-scale winter Nighttime PM_{2.5} concentrations and population exposure using SDGSAT-1 glimmer imagery. IEEE J. Sel. Top. Appl. Earth Observ. Remote Sens. 18, 1626–1637.
- Lu, S., Xiao, Y., Lu, Y., Lin, J., 2024. Spatialization of electricity consumption by combining high-resolution nighttime light remote sensing and urban functional zoning information. Geo-spat. Inf. Sci. 1–14.
- Luo, E., Kuffer, M., Wang, J., 2022. Urban poverty maps from characterising deprivation using geo-spatial data to capturing deprivation from space. Sustain. Cities Soc. 84, 104033.
- Ma, T., Zhou, C., Pei, T., Haynie, S., Fan, J., 2014. Responses of Suomi-NPP VIIRSderived nighttime lights to socioeconomic activity in China's cities. Remote Sens. Lett. 5, 165–174.
- Ma, L., Che, X., Zhang, J., Fang, F., Chen, M., 2019. Rural poverty identification and comprehensive poverty assessment based on quality-of-life: the case of Gansu Province (China). Sustainability 11, 4547.
- Meng, Y., Xing, H., Yuan, Y., Wong, M.S., Fan, K., 2020. Sensing urban poverty: from the perspective of human perception-based greenery and open-space landscapes. Comput. Environ. Urban. Syst. 84, 101544.
- Muñetón-Santa, G., Manrique-Ruiz, L.C., 2023. Predicting multidimensional poverty with machine learning algorithms: an open data source approach using spatial data. Sociol. Sci. 12, 296.
- Ni, Y., Li, X., Ye, Y., Li, Y., Li, C., Chu, D., 2021. An investigation on deep learning approaches to combining Nighttime and daytime satellite imagery for poverty prediction. IEEE Geosci. Remote Sensing Lett. 18, 1545–1549.
- Niu, T., Chen, Y., Yuan, Y., 2020. Measuring urban poverty using multi-source data and a random forest algorithm: a case study in Guangzhou. Sustain. Cities Soc. 54, 102014.
- Pan, J., Hu, Y., 2018. Spatial identification of multi-dimensional poverty in rural China: a perspective of Nighttime-light remote sensing data. J. Indian Soc. Remote Sens. 46, 1–19.
- Pandey, B., Brelsford, C., Seto, K.C., 2022. Infrastructure inequality is a characteristic of urbanization. Proc. Natl. Acad. Sci. USA 119, e2119890119.
- Pokhriyal, N., Jacques, D.C., 2017. Combining disparate data sources for improved poverty prediction and mapping. Proc. Natl. Acad. Sci. USA E9783–E9792.
- Putri, S.R., Wijayanto, A.W., Sakti, A.D., 2022. Developing relative spatial poverty index using integrated remote sensing and geospatial big data approach: a case study of East Java. Indonesia. IJGI 11, 275.
- Puttanapong, N., Martinez Jr., A.M., Addawe, M., Bulan, J., Durante, R.L., Martillan, M., 2022. Predicting poverty using geospatial data in Thailand. ISPRS Int. J. Geo Inf. 11, 293.
- Qiu, S., Chen, Z., Luo, H., Lin, J., Lu, S., Zhang, X., 2024. Evaluation of impervious surface extraction based on Qimingxing-1 nighttime light and point of interest data. International Journal of Digital Earth 17, 2430680.
- Rybnikova, N., Portnov, B.A., 2020. Testing the generality of economic activity models estimated by merging night-time satellite images with socioeconomic data. Adv. Space Res. 66, 2610–2620.
- Sanchez de Miguel, A., Kyba, C.C.M., Zamorano, J., Gallego, J., Gaston, K.J., 2020. The nature of the diffuse light near cities detected in nighttime satellite imagery. Sci. Rep. 10, 7829.
- Schimmel, J., 2009. Development as happiness: the subjective perception of happiness and UNDP'S analysis of poverty, Wealth and Development. J. Happiness Stud. 10, 93–111.
- Shi, K., Chang, Z., Chen, Z., Wu, J., Yu, B., 2020. Identifying and evaluating poverty using multisource remote sensing and point of interest (POI) data: a case study of Chongqing, China. J. Clean. Prod. 255, 120245.
- Stokes, E.C., Roman, M.O., 2022. Tracking COVID-19 urban activity changes in the Middle East from nighttime lights. Sci. Rep. 12, 8096.
- Su, S., Gong, Y., Tan, B., Pi, J., Weng, M., Cai, Z., 2017. Area social deprivation and public health: Analyzing the spatial non-stationary associations using geographically weighed regression. Soc. Indic. Res. 133, 819–832.
- Tan, Y., Wu, P., Zhou, G., Li, Y., Bai, B., 2020. Combining residual neural networks and feature pyramid networks to estimate poverty using multisource remote sensing data. IEEE Journal of Selected Topics in Applied Earth Observations and Remote Sensing 13, 553–565.
- Tang, W., Chakeri, A., Krim, H., 2022. Discovering urban functional zones from biased and sparse points of interests and sparse human activities. Expert Syst. Appl. 207, 118062.
- Wang, W., Cheng, H., Zhang, L., 2012. Poverty assessment using DMSP/OLS night-time light satellite imagery at a provincial scale in China. Adv. Space Res. 49, 1253–1264.
- Wang, C., Xu, W., Chen, Z., Liu, S., Li, W., Zhang, L., Gao, S., Huang, Y., Wu, J., Yu, B., 2025a. STARS: a novel gap-filling method for SDGSAT-1 nighttime light imagery using spatiotemporal and spectral synergy. Remote Sens. Environ. 322, 114720.
- Wang, Y., Huang, H., Wu, B., 2025b. Evaluating the potential of SDGSAT-1 glimmer imagery for urban road detection. IEEE J. Sel. Top. Appl. Earth Observ. Remote Sens. 18, 785–794.
- Wei, W., Zhang, X., Cao, X., Zhou, L., Xie, B., Zhou, J., Li, C., 2021. Spatiotemporal dynamics of energy-related CO2 emissions in China based on nighttime imagery and land use data. Ecol. Indic. 131, 108132.
- Xiang, H., Xi, Y., Mao, D., Xu, T., Wang, M., Yu, F., Feng, K., Wang, Z., 2023. Modeling potential wetland distributions in China based on geographic big data and machine learning algorithms. Int. J. Digit. Earth 16, 3706–3724.

- Xie, Q., Cai, C., Jiang, Y., Zhang, H., Wu, Z., Xu, J., 2024. Investigating the performance of SDGSAT-1/GIU and NPP/VIIRS nighttime light data in representing nighttime vitality and its relationship with the built environment: a comparative study in Shanghai. China. Ecol. Indic. 160, 111945.
- Xiong, S., Zhang, X., Wang, H., Lei, Y., Tan, G., Du, S., 2025. Mapping the first dataset of global urban land uses with Sentinel-2 imagery and POI prompt. Remote Sens. Environ. 327, 114824.
- Xu, J., Song, J., Li, B., Liu, D., Cao, X., 2021a. Combining night time lights in prediction of poverty incidence at the county level. Appl. Geogr. 135.
- Xu, L., Deng, X., Jiang, Q., Ma, F., 2021b. Identification and alleviation pathways of multidimensional poverty and relative poverty in counties of China. J. Geogr. Sci. 31, 1715–1736
- Xu, Y., Mo, Y., Zhu, S., 2021c. Poverty Mapping in the Dian-Gui-Qian Contiguous Extremely Poor Area of Southwest China Based on Multi-Source Geospatial Data. Sustainability 13, 8717.
- Yin, J., Qiu, Y., Zhang, B., 2021. Identification of poverty areas by remote sensing and machine learning: a case study in Guizhou, Southwest China. ISPRS Int. J. Geo Inf. 10. 11.
- Yu, B., Shi, K., Hu, Y., Huang, C., Chen, Z., Wu, J., 2015. Poverty evaluation using NPP-VIIRS Nighttime light composite data at the county level in China. IEEE J.Sel. Top. Appl. Earth Observations Remote Sensing 8, 1217–1229.
- Yu, B., Chen, F., Ye, C., Li, Z., Dong, Y., Wang, N., Wang, L., 2023. Temporal expansion of the nighttime light images of SDGSAT-1 satellite in illuminating ground object extraction by joint observation of NPP-VIIRS and sentinel-2A images. Remote Sens. Environ. 295, 113691.

- Zhang, Q., Levin, N., Chalkias, C., Letu, H., 2015. Nighttime Light Remote Sensing: Monitoring Human Societies from Outer Space.
- Zhang, G., Guo, X., Li, D., Jiang, B., 2019. Evaluating the potential of LJ1-01 Nighttime light data for Modeling socio-economic parameters. Sensors 19, 1465.
- Zhang, D., Cheng, B., Shi, L., Gao, J., Long, T., Chen, B., Wang, G., 2022. A Destriping algorithm for SDGSAT-1 Nighttime light images based on anomaly detection and spectral similarity restoration. Remote Sens 14.
- Zhang, Y., Xu, Y., Gao, J., Zhao, Z., Sun, J., Mu, F., 2025. Urban functional zone identification based on multimodal data fusion: a case study of Chongqing's central urban area. Remote Sens 17, 990.
- Zhao, M., Zhou, Y., Li, X., Zhou, C., Cheng, W., Li, M., Huang, K., 2020. Building a series of consistent night-time light data (1992-2018) in Southeast Asia by integrating DMSP-OLS and NPP-VIIRS. IEEE Trans. Geosci. Remote Sensing 58, 1843–1856.
- Zhao, C., Cao, X., Chen, X., Cui, X., 2022. A consistent and corrected nighttime light dataset (CCNL 1992–2013) from DMSP-OLS data. Sci Data 9, 424.
- Zheng, Q., Seto, K.C., Zhou, Y., You, S., Weng, Q., 2023. Nighttime light remote sensing for urban applications: Progress, challenges, and prospects. ISPRS-J. Photogramm. Remote Sens. 202, 125–141.
- Zheng, X., Zhang, W., Deng, H., Zhang, H., 2024. County-level poverty evaluation using machine learning, Nighttime light, and geospatial data. Remote Sens 16, 962.
- Zhuo, L., Shi, Q., Tao, H., Zheng, J., Li, Q., 2018. An improved temporal mixture analysis unmixing method for estimating impervious surface area based on MODIS and DMSP-OLS data. ISPRS J. Photogramm. Remote Sens. 142, 64–77.